Classification scheme of triply excited states from a molecular viewpoint

S. Watanabe
Observatoire de Paris-Meudon, 92190 Meudon, France

C. D. Lin
Department of Physics, Cardwell Hall, Kansas State University, Manhattan, Kansas 66506
(Received 20 October 1986)

Energy levels of triply excited states of an atom with all three electrons in the same shell are obtained by a model calculation. The nodal pattern of an eigenfunction at the symmetry configuration plays a crucial role in the manifestation of moleculelike modes as in the case of doubly excited states. It is shown that the correlation of the three electrons leads to normal modes isomorphic to those of a molecule with D_{3h} symmetry. The energy levels may be thus regrouped into manifolds, each revealing the rotational level structure of a symmetric top. The validity of the model is discussed in reference to known experimental and theoretical results.

I. INTRODUCTION

The study of doubly excited states has been a central theme in atomic physics over the past two decades. Theoretical investigations of two-electron atoms have revealed systematic features in energy levels and lifetimes controlled by correlations. A large amount of effort has been devoted to seeking a language for describing observed features from a unified viewpoint, resulting in a unification[1] of the hyperspherical analysis of radial correlations[2–7] and the rovibrational description of angular correlations.[8–12] Two-electron correlation patterns are now understood to be isomorphic to the stretching and rovibrational modes of a floppy linear triatomic molecule. The sought language is thus analogous to that of molecular physics, a rather natural consequence in retrospect because the latter came into use precisely for the purpose of describing strong correlations of atoms in a molecule. Although there exist subtle differences between electrons in an atom and atoms in a molecule,[1(a)] the isomorphism tells us why Macek's adiabatic description[2–6] of doubly excited states, modeled after the Born-Oppenheimer treatment of molecules, has been quite successful.

Strong correlations are also expected in triply and multiply excited states. Experimental observations and theoretical studies of these states are scarce so far, but several isolated resonances have been ascribed to temporary formation of triply excited states (Sec. IV). The importance of multiply excited states has been also recognized recently in multiple charge transfer in the collision of highly charged ions with atoms.[13] Progress in experimental and computational technology will undoubtedly reveal a multitude of triply excited states in the near future. It appears thus timely to begin a search for a simple and comprehensive language for classifying and interpreting triply excited states. Instead of studying resonance by resonance, this paper extends previous analyses of doubly excited states to triply excited states and seeks a language capable of treating each manifold of resonances collectively, elucidating the systematics of energy-level positions from a molecular viewpoint.

Identification of moleculelike modes in multiply excited atomic states has been conceptually elusive. Electrons will readily fall away from an equilibrium configuration since it is achieved by the competition between electron-electron repulsion and electron-nucleus attraction, thus intrinsically unstable. However, it should be recognized that the attractiveness of the nucleus causes the electrons to orbit around it, thus the average effective force on the electronic *orbits* rather than the electrons themselves tends to confine the orientational degrees of freedom. As a result, parameters representing the orbits would perform rovibrational motion under the influence of the electron-electron interaction. This argument rationalizes the use of the molecular language for the study of electron correlations.

Although it would be desirable to deduce an effective Hamiltonian for the motion of the electronic orbits, it is not essential to write down such a Hamiltonian explicitly for observing moleculelike modes of multiply excited states and predicting qualitatively correct energy ordering. We demonstrate moleculelike modes by analyzing the angular correlations of triply excited states in a model three-electron problem. The model assumes that the *average* radial distances of the electrons are equal, which is tantamount to restricting their radial degrees of freedom while leaving the orientational degrees of freedom unconstrained.[11] This model is introduced as an approximation to the variational diagonalization of the three-electron Hamiltonian in such a manner that its systematic improvement may be readily foreseen. Although limited by the neglect of radial correlations, this type of model permits us to sort out dominant effects of angular correlations which shape the level structure of triply excited states in a given quantum shell. We will regroup the energy levels of this model into manifolds according to the nodal patterns of the eigenfunctions at the symmetric equilibrium configuration. We shall classify the resultant manifolds from a molecular viewpoint rendering a global understanding of three-electron correlations. Specifically,

we show that energy levels of each manifold reveal a structure analogous to that of a symmetric top while different manifolds are characterized by different vibrational modes.

This article is organized as follows. Section II A formulates the model clarifying each step of our approximation, Sec. II B discusses a method for computing energy levels and eigenfunctions, and Sec. II C presents the resulting levels, using only the standard configuration labels, and points out the limitation of this representation. Section III introduces an alternative viewpoint analogous to molecular physics which permits us to see the rovibrational level structure resembling that of a molecule with the D_{3h} symmetry. Section IV discusses the implication and validity of the present study in reference to the previously calculated or observed triply excited resonances of He^-. Section V concludes the paper with a brief discussion on radial correlations, pointing out the present work's implications on triply excited states of multielectron atoms.

II. MODEL THREE-ELECTRON PROBLEM

A. Description of the model

As noted in the Introduction, the collective modes of the three electrons in an atom pertain to the motion of their orbits rather than to the localized oscillations of the electrons themselves. In order to take this fact into account, we derive our model from an approximation of the quasibound states by the restricted intrashell configuration-interaction (CI) wave functions of the form

$$\Psi^{LS}_{NZ*}(\mathbf{r}_1,\mathbf{r}_2,\mathbf{r}_3)=\sum_{l_1l_2l_3,L_{12},S_{12}} C^{L_{12}S_{12}}_{l_1l_2l_3}\left[\sum_P(-1)^P P\psi^{L_{12}S_{12}}_{l_1l_2l_3}(\mathbf{r}_1,\mathbf{r}_2,\mathbf{r}_3)\right], \tag{1}$$

where L and S are total angular momentum and spin, respectively, N is the principal quantum number of the shell, Z^* is the effective charge to be determined shortly, and P denotes a permutation operator of S_3. Here $\psi^{L_{12}S_{12}}_{l_1l_2l_3}(\mathbf{r}_1,\mathbf{r}_2,\mathbf{r}_3)$ is an unsymmetrized basis function defined by

$$\psi^{L_{12}S_{12}}_{l_1l_2l_3}(\mathbf{r}_1,\mathbf{r}_2,\mathbf{r}_3)=f_{Nl_1}(r_1)f_{Nl_2}(r_2)f_{Nl_3}(r_3)\times\phi^{L_{12}M}_{l_1l_2l_3}(\hat{\omega})\chi^{S_{12}}(1,2,3) \tag{2}$$

with

$$\phi^{L_{12}M}_{l_1l_2l_3}(\hat{\omega})=[[Y_{l_1}(\hat{\mathbf{r}}_1)Y_{l_2}(\hat{\mathbf{r}}_2)]^{(L_{12})}Y_{l_3}(\hat{r}_3)]^{(L)}_M , \tag{3}$$

$$\chi^{S_{12}}(1,2,3)=[[\chi(1)\chi(2)]^{(S_{12})}\chi(3)]^{(s)} , \tag{4}$$

where in (2) $f_{Nl}(r)$ is the Coulomb radial wave function with the effective charge Z^* and L_{12} and S_{12} are intermediate angular momentum and spin $\mathbf{L}_{12}=\mathbf{l}_1+\mathbf{l}_2$ and $\mathbf{S}_{12}=\mathbf{s}_1+\mathbf{s}_2$, respectively. In (3) and henceforth, $\hat{\omega}$ denotes $\hat{\mathbf{r}}_1$, $\hat{\mathbf{r}}_2$, and $\hat{\mathbf{r}}_3$ collectively, and χ in (4) denotes a spin function.

The three-electron Hamiltonian reads

$$H=H_0+V_{e\text{-}e} \tag{5}$$

with

$$H_0=\sum_{i=1}^{3}\left[-\tfrac{1}{2}\nabla_i^2-\frac{Z}{r_i}\right], \tag{6}$$

$$V_{e\text{-}e}=\frac{1}{r_{12}}+\frac{1}{r_{23}}+\frac{1}{r_{31}} . \tag{7}$$

Because we use a unique effective charge Z^* for all the three electrons, the expectation value of H_0 with respect to the wave function (1) is

$$\langle H_0\rangle=(\Psi^{LS}_{NZ*}\mid H_0\mid\Psi^{LS}_{NZ*})/(\Psi^{LS}_{NZ*}\mid\Psi^{LS}_{NZ*})=-\frac{3Z^*}{2N^2}(2Z-Z^*) , \tag{8}$$

which is independent of the angular and spin quantum numbers. In order to estimate Z^*, let us evaluate the expectation value of the electron-electron interaction potential $V_{e\text{-}e}$ approximately and minimize the total energy with respect to Z^*. To this end, consider an equilateral triangle formed by the three electrons with the nucleus at its center. We approximate $\langle V_{e\text{-}e}\rangle$ by the expectation value at this configuration, thus

$$\langle V_{e\text{-}e}\rangle\simeq 3\left\langle\frac{1}{\sqrt{3}r}\right\rangle=\sqrt{3}Z^*/N^2 , \tag{9}$$

where r is the distance of each electron from the nucleus. Adding (8) and (9) and minimizing with respect to Z^*, we get

$$Z^*=Z-1/\sqrt{3} \tag{10}$$

and

$$E=-3Z^*/2N^2 . \tag{11}$$

Equation (11) is the quantized energy of a three-electron system in the field of a nucleus with effective charge Z^*. The rest of the paper examines, in essence, the departure of $\langle V_{e\text{-}e}\rangle$ from this simple estimate, while holding $\langle H_0\rangle$ and Z^* as given by (8) and (10), respectively.

Although we can evaluate the expectation value of $V_{e\text{-}e}$ rigorously using wave function (1), we employ a simplification similar to that employed in the rigid bender model.[11] Recalling that (9) is equivalent to replacing the radial distance of each electron by

$$\bar{r}=N^2/Z^* , \tag{12}$$

we set $r_1=r_2=r_3=\bar{r}$ in $V_{e\text{-}e}$ but without restricting the angular degrees of freedom. Consequently, the variational procedure requires us to diagonalize this effective potential $\bar{V}_{e\text{-}e}$ using the angular and spin basis functions (3) and (4). The approximate total energy is then

$$E_{\rm app}=\langle H_0\rangle+\langle \bar{V}_{e\text{-}e}\rangle=-\frac{3Z^*}{2N^2}(2Z-Z^*)+\langle \bar{V}_{e\text{-}e}\rangle \ . \tag{13}$$

Before going further, let us comment on some obvious limitations of the model. Firstly, fixing the screened charges of all the three electrons to a unique constant Z^* does not represent the radial correlation fully. In a real system the effective charge of each electron fluctuates about Z^*. Inclusion of such fluctuations is what is normally done by the full CI calculation. Secondly, if basis functions representing such fluctuations were included, $\langle H_0\rangle$ would no longer be independent of the angular and spin quantum numbers. Omitting this effect becomes a good approximation when Z is so large that $V_{e\text{-}e}$ may be treated perturbatively. In contrast, $\langle H_0\rangle$ is expected to depend on the angular and spin correlations in negative ions. Our model neglects this fact entirely. Thirdly, replacing r_i by $\bar{r}$ neglects the dependence of the size of an electronic orbit on its eccentricity. Thus $\langle V_{e\text{-}e}\rangle$ as evaluated with this restriction does not reflect subtle effects such as the rotational contraction of the system.[1(a)] Lastly, replacing $\bar{r}$ by N^2/Z^* is an underestimate because the repulsion becomes stronger as the configuration of the three electrons deviates from the equilateral triangle considered above. Despite these limitations our model is sufficiently realistic for predicting the qualitatively correct behavior of the system (Sec. IV).

B. Computational procedure

Let us describe in some detail how the matrix elements are evaluated. For computational convenience, we order the angular momenta l_1,l_2,l_3 as follows.

(i) If all l's are different, then $l_1<l_2<l_3$.

(ii) If any pair of l's are identical, then we set $l_1=l_2$ regardless of l_3.

The permutation group S_3 possesses six permutations, each belonging to one of the following three equivalence classes.

(i) Class 1, consisting of the identity e.

(ii) Class 2, consisting of the transpositions (12), (23), and (31).

(iii) class 3, consisting of the cyclic permutations (123) and $(123)^2$.

This fact will be referred to in the subsequent discussions. Calculating the matrix elements of operators such as (23), $1/r_{23},\ldots$ necessitates recoupling of the angular momenta as well as spins because our basis functions are adapted to the intermediate coupling of l_1 and l_2 and of $\mathbf{S}_1$ and $\mathbf{S}_2$. Let us demonstrate the recoupling technique using operator (23) as an example. Now consider the equation

$$(23)\phi^{L_{12}M}_{l_1l_2l_3}(\hat{\omega})=\phi^{L_{12}M}_{l_1l_2l_3}(\hat{\mathbf{r}}_1,\hat{\mathbf{r}}_3,\hat{\mathbf{r}}_2)$$
$$=\sum_{L_{23},L_{13}}((l_1l_2)L_{12},l_3\mid l_1,(l_2l_3)L_{23})(-1)^{l_2+l_3-L_{23}}(l_1,(l_3l_2)L_{23}\mid(l_1l_3)L_{13},l_2)\phi^{L_{13}M}_{l_1l_3l_2}(\hat{\omega}) \ . \tag{14}$$

The last expression results from three steps. The first step goes to the coupling of l_2 and l_3. The second step is to interchange $\hat{\mathbf{r}}_3$ and $\hat{\mathbf{r}}_2$, which gives rise to the interchange of l_3 and l_2 and the phase $(-1)^{l_2+l_3-L_{23}}$. The third step couples l_1 and l_3. Equation (14) leads to

$$(\phi^{L_{12}M}_{l_1l_2l_3}(\hat{\omega})\mid(23)\mid\phi^{L_{12}M}_{l_1l_2l_3}(\hat{\omega}))=\delta_{l_2l_3}\sum_{L_{23},L_{13}}((l_1l_2)L_{12},l_3\mid l_1,(l_2l_3)L_{23})(-1)^{l_2+l_3-L_{23}}(l_1,(l_3l_2)L_{23}\mid(l_1l_3)L_{13},l_2)\delta_{L_{13},L_{12}} \ . \tag{15}$$

TABLE I. Matrix representation of the permutation operators for the doublet state with respect to the basis vector

$$\begin{bmatrix}\chi^1(1,2,3)\\ \chi^0(1,2,3)\end{bmatrix},$$

where χ^1 and χ^0 are triplet and singlet parent spin functions Eq. (4). The corresponding matrices for the quartet state are one dimensional and are identically 1 with respect to χ^1.

e	(123)	$(123)^2$	(12)	(23)	(31)
$\begin{bmatrix}1&0\\0&1\end{bmatrix}$	$\begin{bmatrix}-\frac{1}{2}&\frac{\sqrt{3}}{2}\\-\frac{\sqrt{3}}{2}&-\frac{1}{2}\end{bmatrix}$	$\begin{bmatrix}-\frac{1}{2}&-\frac{\sqrt{3}}{2}\\\frac{\sqrt{3}}{2}&-\frac{1}{2}\end{bmatrix}$	$\begin{bmatrix}1&0\\0&-1\end{bmatrix}$	$\begin{bmatrix}-\frac{1}{2}&\frac{\sqrt{3}}{2}\\\frac{\sqrt{3}}{2}&\frac{1}{2}\end{bmatrix}$	$\begin{bmatrix}-\frac{1}{2}&-\frac{\sqrt{3}}{2}\\-\frac{\sqrt{3}}{2}&\frac{1}{2}\end{bmatrix}$

The matrix elements of the permutation operators with respect to spin functions (4) are well known; the principle of evaluation being identical to that of the angular part. The result[14] is reproduced in Table I for later use.

This technique permits us to calculate the overlap and potential energy matrices. However, some of the antisymmetrized basis functions are identically zero or linearly dependent, particularly when $l_1=l_2=l_3$. To avoid spurious eigenvalues in a specific numerical calculation, it is essential to deduce the number of linearly independent basis functions explicitly. We do so by following Clark and Greene.[15] The cases $l_1\neq l_2\neq l_3$ and $l_1=l_2\neq l_3$ are trivial. The first case $l_1\neq l_2\neq l_3$ gives one quartet and two doublet ($S_{12}=0$ and 1) states and the second case $l_1=l_2\neq l_3$ gives one quartet and one doublet ($S_{12}=1$) state if $(-1)^{l_1+l_2-L_{12}}=1$ but only one doublet ($S_{12}=0$) if $(-1)^{l_1+l_2-L_{12}}=-1$. If $l_1=l_2=l_3=l$, then the set of normalized functions:

$$\{\Phi^{L_{12}M}_{l_1l_2l_3}(\hat{\omega})\chi^{S_{12}}(1,2,3)\}\ , \tag{16}$$

transforms onto itself under any permutation operation where $0\leq L_{12}\leq 2l$. $S_{12}=1$ for quartet and $S_{12}=0$ and 1 for doublet. According to the group theory, the number n of nontrivial vectors belonging to a particular irreducible representation is obtained by[16]

$$n=\frac{1}{h}\mathbf{P}\cdot\mathbf{Q}\ , \tag{17}$$

where h is the order of the group (equal to 6 here), and $\mathbf{P}$ represents the characters of the permutation operators in the vector space (16), and $\mathbf{Q}$ represents the characters of the permutation operators in the irreducible representation of interest which is A_2, the totally antisymmetric representation. Accordingly, $\mathbf{Q}$ consists of the following elements: 1 for the first class with the identity and also for the third class with the cyclic permutations, -1 for the second class with the three transpositions. Hence, Eq. (17) reads explicitly as

$$n=\tfrac{1}{6}\sum_{L_{12},S_{12}}(\phi^{L_{12}M}_{l_1l_2l_3}(\hat{\omega})\chi^{S_{12}}(123)\,|\,1\times e-3\times(12)+2\times(123)\,|\,\phi^{L_{12}M}_{l_1l_2l_3}(\hat{\omega})\chi^{S_{12}}(123))\ , \tag{17'}$$

employing e, (12), and (123) as the representative elements of the three classes. n may thus be evaluated readily using the recoupling technique described above. The total number of nontrivial eigenvectors of $H_{\rm eff}$ may be obtained in this manner and used to monitor the reliability of the numerical orthogonalization procedure.

C. Energy levels of the model

By imposing the form (1) on the CI wave functions, we committed ourselves to describing intrashell states only. However, as is well known from the study of doubly excited states, some states have a sizable contribution to the angular correlation energy from virtual orbitals whose angular momenta may exceed the upper limit of the intrashell angular momenta, namely $N-1$. For example, in the $N=2$ shell, the intrashell configuration $2p^3\,{}^4S^o$ mixes with the configuration $2p3\bar{d}^2\,{}^4S^o$ where $3\bar{d}$ represents a virtual or polarized d orbital which sharpens the angular correlation. For this reason it is necessary to make a mock-up part of the effect due to virtual orbitals in our model calculation. Here we choose the basis set for which the maximum angular momentum permitted for each electron is $l_{\max}=N$. However, we exclude higher angular momenta in order to avoid exaggerating the intershell effect. We carry out a separate calculation in which $l_{\max}=N-1$ in order to identify the genuine intrashell states. The results to be presented below as well as in Sec. IV exclude in this manner artificially produced intershell states. The total angular momentum of an intrashell state is always limited by $3N-3$, and the parity of the states, for which the total angular momentum is the maximum $L=3N-3$, must always be $(-1)^L$.

We show in Fig. 1 the energy levels of the $N=3$ shell of He^-. The presentation and discussion of the result for the $N=2$ shell are postponed until Sec. IV. In Fig. 1 the horizontal axis labels symmetries by the good quantum numbers L, S, and π. The vertical axis gives the absolute energy in atomic units measured from the triple ionization limit. It should be noted that the energy of the ground state of He is -2.9035 a.u. relative to the triple ionization limit. The formula

$$\varepsilon_{\rm eV}=27.21\times(2.9035+\varepsilon_{\rm a.u.}) \tag{18}$$

converts the energy position from a.u. into eV in a collision of electrons with $He(1s^2\,{}^1S^e)$.

The energy levels in this map show no obvious systematics. It appears rather hopeless to gain any insight

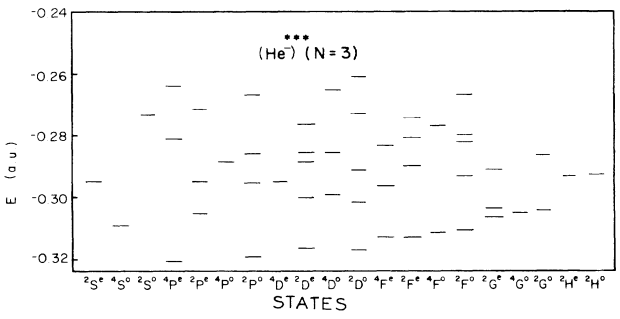

FIG. 1. Levels obtained by the model calculation for the $N=3$ shell of He^-. States are labeled by L, S, and π (horizontal axis) and the energy is measured from the triple ionization threshold in a.u. (vertical axis).

into the three-electron correlation patterns unless we modify our picture and adopt a more transparent representation.

III. MOLECULAR INTERPRETATION OF TRIPLY EXCITED STATES

A. Body-frame analysis of wave functions

Let us notice that the symmetry properties of an eigenfunction stem from the symmetry of the system, thus are independent of the model. We first study the symmetry properties of the general three-electron system, then see if these properties are reflected in the energy-level structure of Fig. 1. Because this article employs atomic physics language, we feel it is necessary to work out the analysis of the symmetry properties explicitly even at the risk of repeating some facts familiar in molecular physics. A natural equilibrium configuration of the three electrons whose dynamics is governed by Hamiltonian (5) is an equilateral triangle with the nucleus at the center. The fact that the inversion-permutation group and the D_{3h} point group acting on this configuration are isomorphic[17] suggests a correspondence between the energy-level structure of triply excited states and that of a D_{3h} molecule.

Let us apply the body-frame analysis of Watanabe and Lin[1(a)] to the three-electron system. First let us define our body frame. As the z axis we take a totally antisymmetric vector

$$\mathbf{S}_z=\mathbf{r}_1\times\mathbf{r}_2+\mathbf{r}_2\times\mathbf{r}_3+\mathbf{r}_3\times\mathbf{r}_1 \ , \tag{19a}$$

which is orthogonal to the plane spanned by the electrons. As the other two axes of the body frame, we take

$$\mathbf{S}_y=\frac{\sqrt{3}}{2}(\mathbf{r}_1-\mathbf{r}_2) \ , \tag{19b}$$

$$\begin{aligned}\mathbf{S}'_x=\mathbf{S}_y\times\mathbf{S}_z=\frac{\sqrt{3}}{2}[&2\mathbf{r}_3-\mathbf{r}_1-\mathbf{r}_2-2(\mathbf{r}_1\cdot\mathbf{r}_2)\mathbf{r}_3\\&+(\mathbf{r}_3\cdot\mathbf{r}_1-\mathbf{r}_1\cdot\mathbf{r}_2-\mathbf{r}_2\cdot\mathbf{r}_3)\mathbf{r}_1\\&+(-\mathbf{r}_3\cdot\mathbf{r}_1-\mathbf{r}_1\cdot\mathbf{r}_2+\mathbf{r}_2\cdot\mathbf{r}_3)\mathbf{r}_2] \ .\end{aligned} \tag{19c}$$

At the symmetric configuration where $\hat{\mathbf{r}}_1\cdot\hat{\mathbf{r}}_2=\hat{\mathbf{r}}_2\cdot\hat{\mathbf{r}}_3=\hat{\mathbf{r}}_3\cdot\hat{\mathbf{r}}_1$, vector $\mathbf{S}'_x$ is proportional to

$$\mathbf{S}_x=\mathbf{r}_3-\tfrac{1}{2}(\mathbf{r}_1+\mathbf{r}_2) \ . \tag{19d}$$

B. Symmetry properties of rotational components

Let us analyze the behavior of wave function (1) at the symmetric configuration. The angular function may be cast into a form revealing rotational components explicitly,

$$\Phi_M^{S_{12}}(\hat{\omega})=\sum_{Q=-L}^{L}\Phi_Q^{S_{12}}(\hat{\omega}')D_{QM}^{(L)}(\hat{\Omega}) \ , \tag{20}$$

where

$$\Phi_M^{S_{12}}(\hat{\omega})=\sum_{l_1,l_2,l_3,L_{12}}C_{l_1l_2l_3}^{L_{12}S_{12}}\phi_{l_1l_2l_3}^{L_{12}M}(\hat{\omega}) \tag{20'}$$

for short-hand notation, and $\hat{\omega}'$ denotes the directional vectors $\hat{\mathbf{r}}'_1$, $\hat{\mathbf{r}}'_2$ and $\hat{\mathbf{r}}'_3$ defined in the body frame $(\mathbf{S}_x,\mathbf{S}_y,\mathbf{S}_z)$, $\hat{\Omega}$ denotes the set of Euler angles for the transformation between the laboratory and body frames, and Q is the projection of L onto the body axis $\hat{\mathbf{S}}_z$, namely $Q=\boldsymbol{L}\cdot\hat{\mathbf{S}}_z$. Note that there are only three degrees of freedom in $\hat{\omega}'$ since the orientation of the body is expressed by $\hat{\Omega}$.

Let us study the transformation properties of each rotational component of (20) under inversion and permutations. First, under the inversion $\mathbf{r}\rightarrow-\mathbf{r}$, the frame vectors transform as

$$\begin{aligned}&\mathbf{S}_x\rightarrow-\mathbf{S}_x \ ,\\&\mathbf{S}_y\rightarrow-\mathbf{S}_y \ ,\\&\mathbf{S}_z\rightarrow\mathbf{S}_z \ ,\end{aligned} \tag{21}$$

which is nothing but a rotation of the original frame by π radians about the $\mathbf{S}_z$ axis. Thus

$$D_{QM}^{(L)}(\hat{\Omega})\rightarrow(-1)^Q D_{QM}^{(L)}(\hat{\Omega}) \quad \text{(inversion)} \ . \tag{22}$$

The $\mathbf{r}_1,\mathbf{r}_2,\mathbf{r}_3$ vectors transform to the positions which are the mirror image of the original vectors with respect to the plane of the three electrons. Therefore, the property

$$Y_l^m(\pi-\theta,\phi)=(-1)^{l+m}Y_l^m(\theta,\phi)$$

leads to

$$\Phi_Q^{S_{12}}(\hat{\omega}')\rightarrow\pi(-1)^Q\Phi_Q^{S_{12}}(\hat{\omega}') \quad \text{(inversion)} \ , \tag{23}$$

where $\pi=(-1)^{l_1+l_2+l_3}$ is the parity of the system. Wave function (1) thus acquires the phase π as it should.

Let us next illustrate the geometrical significance of each permutation through the example of transposition (23), restricting ourselves to the D_{3h} symmetric configuration. The following discussion applies to states whose eigenfunctions do not vanish identically at this configuration. A discussion for more general cases will be given in Sec. III C 1. Figure 2 illustrates that the effect of (23) on the frame is equivalent to a rotation by π about

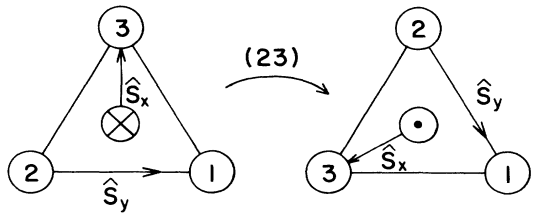

FIG. 2. Diagram showing the effect of the transposition (23) on the body frame and the position vectors $\mathbf{r}'_1$, $\mathbf{r}'_2$, and $\mathbf{r}'_3$. To the right, the unpermuted vectors; $\odot$ and $\otimes$ mean that S_z is out of and into the plane, respectively. The plane does not necessarily contain the nucleus.

the y axis followed by a rotation by $-2\pi/3$ about the new z axis. On the other hand, the transformed vectors $\mathbf{r}_1'$, $\mathbf{r}_2'$, and $\mathbf{r}_3'$ may be reflected with respect to the plane of the electrons to recover their original relationship with the body frame. Hence

$$D^{(L)}_{QM}(\hat{\Omega}) \rightarrow (-1)^{L+Q} e^{i(2\pi Q/3)} D^{(L)}_{-QM}(\hat{\Omega}) , \tag{24}$$

and

$$\Phi^{S_{12}}_{Q}(\hat{\omega}') \rightarrow \pi(-1)^{Q} \Phi^{S_{12}}_{Q}(\hat{\omega}') . \tag{25}$$

Table II summarizes the symmetry properties of these functions for all the permutations. Substituting the results of Tables I and II into (1), we can readily rewrite the antisymmetrized basis function at the symmetric configuration in terms of the rotor and internal functions. We have

TABLE II. Symmetry properties of the rotor function and body-frame wave function under reflection with respect to the plane and permutations.

Operator	$D^{(L)}_{QM}(\hat{\Omega})$	$\Phi^{S_{12}}_{Q}(\hat{\omega}')$
e	$\delta_{QQ'}$	1
(123)	$e^{i(2\pi/3)Q}\delta_{QQ'}$	1
$(123)^2$	$e^{-i(2\pi/3)Q}\delta_{QQ'}$	1
(12)	$(-1)^{L+Q}\delta_{-QQ'}$	$\pi(-1)^{Q}$
(23)	$(-1)^{L+Q}e^{i(2\pi/3)Q}\delta_{-QQ'}$	$\pi(-1)^{Q}$
(31)	$(-1)^{L+Q}e^{-i(2\pi/3)Q}\delta_{-QQ'}$	$\pi(-1)^{Q}$
Reflection with respect to plane	1	$\pi(-1)^{Q}$

$$\sum_{l_1 l_2 l_{3i}, L_{12} S_{12}} C^{L_{12} S_{12}}_{l_1 l_2 l_3} \sum_{P} (-1)^{P} P \psi^{L_{12} S_{12}}_{l_1 l_2 l_3}(\mathbf{r}_1, \mathbf{r}_2, \mathbf{r}_3) \propto \sum_{Q} \tilde{D}^{L\eta-}_{QM}(\hat{\Omega}) \left[1 + 2\cos\left[\frac{2\pi Q}{3}\right] \right] \Phi^{1}_{Q}(\hat{\omega}') \chi^{1}(1,2,3) \text{ for } S=\tfrac{3}{2} ,$$

$$\sum_{Q} \tilde{D}^{L\eta-}_{QM}(\hat{\Omega}) \left\{ \left[1 - \cos\left[\frac{2\pi Q}{3}\right] \right] \Phi^{1}_{Q}(\hat{\omega}') \chi^{1}(1,2,3) + i\sqrt{3} \sin\left[\frac{2\pi Q}{3}\right] \Phi^{0}_{Q}(\omega') \chi^{0}(1,2,3) \right\} \text{ for } S=\tfrac{1}{2},\ S_{12}=1 , \tag{26}$$

$$\sum_{Q} \tilde{D}^{L\eta+}_{QM}(\hat{\Omega}) \left\{ -i\sqrt{3} \sin\left[\frac{2\pi Q}{3}\right] \Phi^{1}_{Q}(\omega') \chi^{1}(1,2,3) + \left[1 - \cos\left[\frac{2\pi Q}{3}\right] \right] \Phi^{0}_{Q}(\omega') \chi^{0}(1,2,3) \right\} \text{ for } S=\tfrac{1}{2},\ S_{12}=0 ,$$

where $\eta = \pi(-1)^{L}$ and

$$\tilde{D}^{L\eta\pm}_{QM}(\hat{\Omega}) = D^{(L)}_{QM}(\hat{\Omega}) \pm \eta D^{(L)}_{-QM}(\hat{\Omega}) . \tag{27}$$

Equations (26) and (27) play a key role in interpreting the energy-level structure in Sec. III C below.

Let us also note the relationship

$$\Phi^{S_{12}}_{-Q}(\hat{\omega}') = \eta(-1)^{Q} \left[\Phi^{S_{12}}_{Q}(\hat{\omega}') \right]^{*} , \tag{28}$$

which follows from the properties of the $3j$ symbols where $*$ denotes the "complex conjugation." Accordingly, the two rotational components Q and $-Q$ of an eigenstate are energetically degenerate. We employ a label $T = |Q|$ in what follows. This quantity T is not an *a priori* good quantum number, but its close connection with the nodal structure of an eigenfunction at the symmetric configuration makes a particular T component stand out. Thus T is expected to be an approximately good quantum number [a similar connection was noted in Ref. 1(a) for doubly excited states]. This is evidenced in the energy-level structure that we now discuss.

C. Moleculelike modes of triply excited states

1. *Rearrangement of energy levels into rovibrational manifolds*

We now regroup the levels of Fig. 1 into manifolds. Each manifold consists of states whose wave functions have a similar nodal pattern. Let us now show that such an arrangement of levels reveals that each manifold resembles a rotational manifold of a molecule with the D_{3h} symmetry. Since the energy levels shown in Fig. 1 include states in which bending vibrational modes are excited, we discuss the level structure manifold by manifold. We start with the manifold whose members are in the vibrational ground state. The angular eigenfunctions of all the members of this manifold should be nodeless at the D_{3h} symmetric configuration. Equation (26) applies leading to the following conditions:

$$\pi(-1)^{T} = + , \tag{29a}$$

$$\eta = - \quad \text{for } T=0 , \tag{29b}$$

and

$$\begin{aligned} &T \equiv 0 \pmod 3 \quad \text{for } S=\tfrac{3}{2} , \\ &T \equiv 1,2 \pmod 3 \quad \text{for } S=\tfrac{1}{2} . \end{aligned} \tag{29c}$$

Condition (29a) means that the internal function $\Phi^{S_{12}}_{Q}(\hat{\omega}')$ has an antinode at the plane of the three electrons containing the nucleus since its sign is unchanged under reflection with respect to the plane (cf. Table II). Condition (29b) assures that the rotor function defined by (27) is nonvanishing when $T=0$. As argued for deducing (24), each permutation induces a rotation of the body frame about the z axis by a multiple of $120° = 2\pi/3$ rad, thus leading to the trigonometric functions in (26) after summing over all permutations. These trigonometric func-

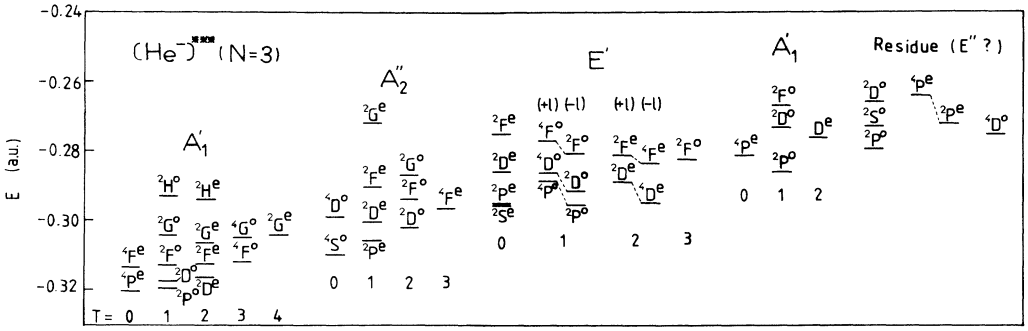

FIG. 3. Levels of Fig. 1 regrouped into moleculelike rotational manifolds. First group for states without nodes in the wave functions. Second group for states with nodes when the nucleus is on the plane of the three electrons. Third group for states corresponding to the doubly degenerate bending mode. Level order of high angular momentum states may not be reliable.

tions interfere destructively unless condition (29c) is met. Gathering the low-lying levels in Fig. 1 which are consistent with (29) leads to a new energy-level pattern of the first group shown in Fig. 3. Here the horizontal axis is labeled by T and the vertical axis by the absolute energy in atomic units relative to the triple ionization limit. This level grouping is similar to the (J,K) grouping of rotational energy levels of a symmetric top except for the fact that there is a rapid truncation in both L and T owing to the constraint of the quantum shell. As illustrated in Fig. 4(a), each state in this manifold pertains to the zero-point fluctuation of the electronic orbits about the equilibrium configuration.

To illustrate the moleculelike behavior further, we also display the rotational energy levels of other manifolds in Fig. 3. The second group consists of the first excited bending vibrational states; the center of charge of the three electrons vibrates with a quantum of energy. The internal wave function $\Phi_Q^{S_{12}}(\hat{\omega}')$ has the odd parity $\pi(-1)^T=-1$ under reflection with respect to the plane. The eigenfunction of a state thus vanishes identically whenever the nucleus lies on the plane.

The discussion of the third manifold motivates to employ the concept of the D_{3h} point group. Let us discuss the D_{3h} symbols. There are six species: A_1', A_2', E', A_1'', A_2'', and E''. The single prime and double prime separate two classes of representation. The single prime pertains to a representation invariant under σ_h, namely the reflection with respect to the plane of the three electrons, and the double prime to a representation which changes sign under σ_h. This parity is given by $\pi(-1)^T$. The symbol A indicates a one-dimensional representation: A_1 is totally symmetric (like the $S=\frac{3}{2}$ spin function) and A_2 totally antisymmetric. The symbol E indicates a two-dimensional representation (like the $S=\frac{1}{2}$ spin function). The full wave function must be totally antisymmetric, that is either of type A_2' or A_2''. The multiplication rule of these symmetry species is straightforward:[17] $A_1\times A_1=A_2\times A_2=A_1$, $A_1\times A_2=A_2$, $A_1\times E=A_2\times E=E$, and $E\times E=E+A_2+A_1$. The D_{3h} classification of rotational states results from the inspection of Table II. The rotational states are one dimensional, A type, if $T\equiv 0 \pmod 3$ and two-dimensional, E type, if $T\not\equiv 0 \pmod 3$. For $T=0$, they are of type A_1 for L even and of type A_2 for L odd [Eq. (24)]. Returning to the first two rotational manifolds of Fig. 3, we note that the first manifold pertains to the one dimensional totally symmetric vibrational state A_1' and the second one to the one dimensional totally antisymmetric vibrational state A_2'' [cf. Table II for the transformation property of $\Phi_Q^{S_{12}}(\hat{\omega}')$]. The third manifold

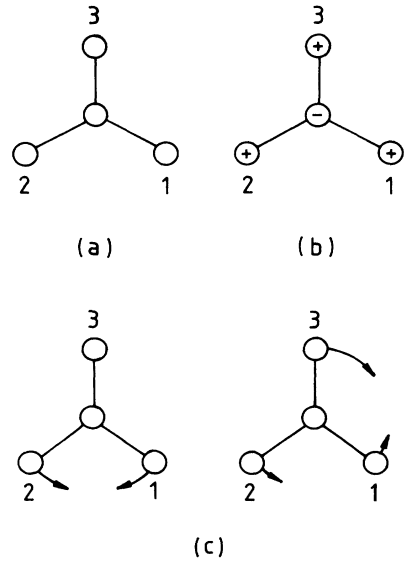

FIG. 4. Graphic representation of molecular bending vibrational modes. The electrons are placed on a sphere; the interaction potential is harmonic and the nucleus is assumed to be massive. (a) A_1' manifold of Fig. 3: The electronic orbits perform zero-point fluctuations about the equilibrium configuration. (b) A_2'' manifold: The electrons and the nucleus move in phase. (c) E' manifold: A pair of degenerate vibrational modes. To the left, two electrons move in phase, the third one being stationary. To the right, the third one moves in phase with the other two moving out of phase.

however pertains to the two-dimensional representation E', doubly degenerate vibrational state, as may be verified using the D_{3h} multiplication rule. This multiplication leads to states labeled E, A_2 and A_1 for $T \neq 0 \pmod 3$. A state labeled A_1 would normally form a K doublet[18] with a state labeled A_2. However, A_1 states are not feasible in this manifold since there is no totally antisymmetric spin function. The K doubling is not explicitly shown in this manifold. On the other hand, an A_2 state and an E state appear as a doublet. This phenomenon is equivalent to the l type doubling in molecular physics caused by the coupling between the rotational and vibrational motion. In the present model the relative level order of l type doublets is opposite to that of NH_3.

The fourth manifold is isomorphic to the first one. Beyond this, states are too scarce for identifying meaningful rotational manifolds. Nonetheless, the rest of the states are arranged in a manner suggestive of the rotational manifold of the E'' vibrational state. A $^4S^e$ state would be the lowest member of the A_2' vibrational state though no $^4S^e$ states are formed in the $N=3$ shell. A_1''-type vibrational states should also manifest themselves in higher quantum shells.

Figure 4 illustrates the vibrational normal modes of the three particles interacting by a harmonic potential on a sphere, (a) being the equilibrium configuration (the nucleus is assumed to be massive). The A_2'' vibrational state corresponds to (b) out-of-phase motion of the nucleus and the three electrons. The E' vibrational state corresponds to the superposition of a pair of degenerate motions (c). On the left, a pair of electrons move in phase, the third one being stationary. On the right, the third electron moves in phase with respect to the other two electrons moving out of phase. If the radial degrees of freedom are relaxed, there appear all together six normal vibrations.[17(b)] One of the three additional modes is the symmetric stretching mode (A_1') and the other two are degenerate vibrational modes (E'). One of the degenerate modes corresponds to the in-phase radial motion of two electrons with the third moving out of phase and the other corresponds to the out-of-phase motion of two electrons with the third approximately stationary [see Fig. 63 of Ref. 17(b), Vol. II].

Let us supplement the discussion by displaying certain sectional views of the probability density distribution (conditional probability distribution plots) integrated over all orientations of the body frame. It is defined for each triply excited state by

$$\rho(r_1,r_2,r_3,\hat{\omega}') = \int |\Psi_{NZ}^{LS*}(\mathbf{r}_1,\mathbf{r}_2,\mathbf{r}_3)|^2 d\hat{\Omega} \ . \tag{30}$$

We set the radial distances r_1, r_2, and r_3 to $\bar{r}$ given by (12). Here the amplitudes of the Coulomb radial functions are roughly the same. In accordance with our model, we evaluate (30) assuming that the radial amplitudes are identical. The maximum probability is normalized to unity for each state. Figs. 5(a) and 5(b) are for the representative states of the three manifolds, namely the $^4P^e$, $^4S^o$, and $^2S^e$ states. For both figures, the positions of two electrons are fixed at $\hat{\mathbf{r}}_2=(90°,120°)$ and $\hat{\mathbf{r}}_3=(90°,-120°)$. In Fig. 5(a) $\hat{\mathbf{r}}_1=(\theta,0°)$ with $0° \leq \theta \leq 90°$, that is electron 1 is placed on the plane which bisects the

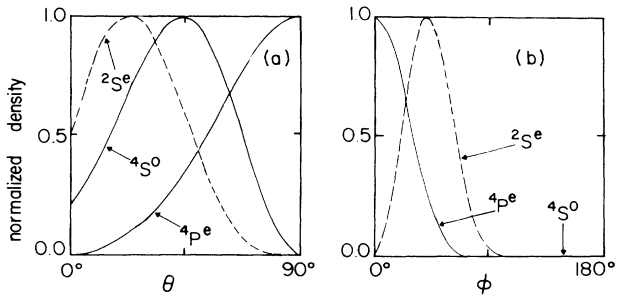

FIG. 5. Conditional probability distribution plots Eq. (30) for the representative states $^4P^e$, $^4S^o$, and $^2S^e$, of the three manifolds of Fig. 3. The position of electron 1 is parametrized by the polar angles (θ,ϕ); the positions of the other electrons are fixed to be $\hat{\mathbf{r}}_2=(90°,120°)$ and $\hat{\mathbf{r}}_3=(90°,-120°)$. (a) for $\hat{\mathbf{r}}_1=(\theta,0°)$, (b) for $\hat{\mathbf{r}}_1=(90°,\phi)$.

$\hat{\mathbf{r}}_{23}$ axis, while in Fig. 5(b) it is placed on the plane containing the nucleus $\hat{\mathbf{r}}_1=(90°,\phi)$ with $0° \leq \phi \leq 180°$. Incidentally, the labels 1, 2, and 3 for the electrons are merely for the sake of discussion and inconsequential because of the antisymmetry of the wave function. The $^4P^e$ state shows a very sharp concentration at the equilibrium configuration $(\theta,\phi)=(90°,0°)$. The $^4S^o$ states has zero probability of being at $\theta=90°$. The $^2S^e$ state has zero probability at $(\theta,\phi)=(90°,0°)$. On the $\theta=90°$ plane, the maximum occurs fairly close to $\phi=0°$, and on the $\phi=0°$ plane the probability maximizes at $\theta \cong 30°$. These sectional views are all in accord with the earlier discussion of molecular modes.

2. *Details of the rotational structure*

A main difference between the three-electron system and an XY_3 molecule should be noted. As is well known, the rotational energy of a prolate (cigar-shaped) molecule increases with T for a fixed L while that of an oblate (pancake-shaped) molecule decreases with T for a fixed L. We notice that the level structure obtained by our model calculation resembles that of a prolate molecule for small L but that of an oblate molecule for larger L ($L > 3$ in the present case). The prolate moleculelike level structure shown in the first group of Fig. 3 disagrees with the energy-level structure obtained by diagonalizing the rigid bender Hamiltonian,

$$H_{\mathrm{RB}} = \frac{1}{2}\frac{1}{\bar{r}^2}(l_1^2+l_2^2+l_3^2) - \frac{3Z}{\bar{r}} + \bar{V}_{e\text{-}e} \ . \tag{31}$$

The lowest manifold of this model is similar to that of an oblate molecule in an electronically symmetric state (not shown).

What causes the low-lying triply excited states to exhibit a prolate rotational level structure? To answer this question let us consider Fig. 6 displaying the conditional probability distributions of the rotational series $^4F^e$, $^2F^o$, $^2F^e$, and $^4F^o$ of the first group of Fig. 3. The setting for this figure is the same as for Fig. 5. The angular positions of the second and the third electrons are set to $\hat{\mathbf{r}}_2=(90°,120°)$ and $\hat{\mathbf{r}}_3=(90°,-120°)$, respectively. Figure 6(a) is a sectional view at $\hat{\mathbf{r}}_1=(\theta,\phi=0°)$ with $0° \leq \theta \leq 90°$;

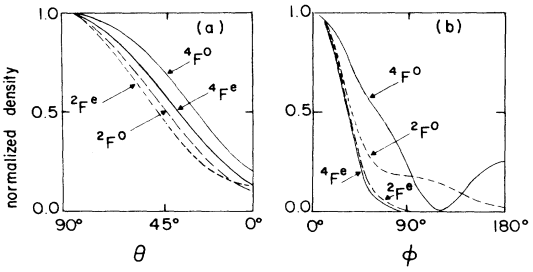

FIG. 6. Sectional views of the conditional probability densities of the rotational series $^4F^e$, $^2F^o$, $^2F^e$, and $^4F^o$ of the first group in Fig. 3. As in Fig. 5, $\hat{\mathbf{r}}_2=(90°,180°)$ and $\hat{\mathbf{r}}_3=(90°,-180°)$. (a) for $\hat{\mathbf{r}}_1=(\theta,0°)$; (b) for $\hat{\mathbf{r}}_1=(90°,\phi)$.

Fig. 6(b) at $\hat{\mathbf{r}}_1=(\theta=90°,\phi)$ with $0°\leq\phi\leq180°$. In Fig. 6(a) the maxima at $\theta=90°$ means that indeed the three electrons tend to be on the plane containing the nucleus. Figure 6(b) shows that on this plane electron 1 prefers the position which makes the three-electron system look like an equilateral triangle, hence like a coplanar oblate molecule. What about the relative energy ordering? Figure 6(b) shows that in the $^4F^e$ state electron 1 has a negligibly small amplitude near the position of the other two electrons, $\phi=\pm120°$, hence it is natural that its energy is the lowest amongst the four states. The observed energy ordering follows from averaging $V_{e\text{-}e}$ over all the possible relative positions of the three electrons. However, the an-

TABLE III. Comparison of our result with the previously calculated or observed energy levels. Experimental and some theoretical levels tabulated originally in eV are converted into a.u. by Eq. (18). Our levels are shifted by 0.1±0.02 a.u. with respect to those of Refs. 32 and 34, except for $^2S^e$. A single asterisk indicates that model may overestimate the effect of virtual orbitals in these states. Double asterisks indicate that these values are obtained by the adiabatic hyperspherical method of Refs. 7 and 36. Uncertainty is estimated from the nonadiabatic correction term.

		Present work	Earlier theoretical works	Experiment
I	$^2P^o$	−0.682	−0.798[d]	
			−0.798[g]	−0.805±0.004[a]
			−0.8278[i]	−0.8113[b]
			−0.79852[m]	−0.801±0.004[c]
			−0.8006[n]	−0.8113[e]
			−0.8179[o]	−0.8032[f]
			−0.795±0.006[s]**	−0.8028±0.002[h]
				−0.801[j]
				−0.8006±0.001[k]
	$^4P^e$	−0.680	−0.7931[p]	
			−0.790±0.008[r]**	
	$^2D^e$	−0.659	−0.761[d]	
			−0.757[g]	−0.765±0.004[a]
			−0.7594[i]	−0.7705[b]
			−0.75602[m]	−0.761±0.004[c]
			−0.7598[n]	−0.7690[e]
			−0.7892[o]	−0.7635±0.001[f]
				−0.7627±0.002[h]
				−0.761[j]
				−0.7609±0.001[k]
II	$^2P^e$	−0.627		
	$^4S^o$	−0.625	−0.7226[p]	
			−0.7221[q]	
			−0.726±0.005[r]**	
	$^2D^o$	−0.592*		
III	$^2P^o$	−0.579	−0.6826[n]	
			−0.6940[o]	
	$^2S^e$	−0.576	−0.7234[n]	−0.720[l]
			−0.7157[o]	
	$^2P^e$	−0.573*		

[a]Reference 19.
[b]Refernce 20.
[c]Reference 21.
[d]Reference 22.
[e]Reference 23.
[f]Reference 24.
[g]Reference 25.
[h]Reference 26.
[i]Reference 27.
[j]Reference 28.
[k]Reference 29.
[l]Reference 30.
[m]Reference 31.
[n]Reference 32.
[o]Reference 33.
[p]Reference 34.
[q]Reference 35.
[r]Reference 7.
[s]Reference 36.

gular correlations of electrons 2 and 3 being not displayed, this restricted set of sectional views is insufficient to account satisfactorily for the $^2F^e$, $^2F^o$, and $^4F^o$ states. In any event, the prolate moleculelike behavior of the low L rotational levels may be attributed to the details of the electron correlations rather than to the shape of the system. Because ours is a model calculation, it remains to be seen whether it represents fine details of the real atomic spectra faithfully. Should the real spectrum resemble that of a prolate or oblate molecule? This can be answered only with the aid of more rigorous calculations or extensive experimental data. Let us note in passing that like a molecule the three electrons tend to concentrate more toward the same plane as T increases except for the $^4F^o$ state [Fig. 6(a)]. Note also that the volume element associated with the probability density distribution is proportional to $d\cos\theta_{12}\ d\cos\theta_{23}\ d\cos\theta_{31}$. The nonnegligible density of the $^2F^o$ state at $\phi=120°$ gets compensated for by the vanishing volume element.

In our model the rotational constant originates entirely from the electron-electron interaction term $V_{e\text{-}e}$. This point leads to the following observation. Using the energy difference of the two rotational states $^2P^o$ and $^2D^o$ of the first manifold, we can estimate the gyroradius R,

$$R=\left[\frac{L(L+1)-L'(L'+1)}{2\Delta\varepsilon}\right]^{1/2}=43 \text{ a.u.}\ , \tag{32}$$

which is much greater than the root-mean-square size of the system $\sqrt{3}r=11$ a.u. Such an overestimate was also found in a similar analysis for doubly excited states of two-electron atoms.[1(a)] Since the rotational splitting in our model is not due to the kinetic energy term as in a molecule, this value of R has nothing to do with the size of the state.

IV. COMPARISON WITH KNOWN RESULTS FOR THE $N=2$ SHELL (REFS. 19–36)

The $N=3$ shell manifolds used for demonstration have been, except for this work, neither computed theoretically nor observed experimentally. Their study remains as a future task. Some states of the $N=2$ shell are known, however, from other calculations and experiments. The results of our model calculation and others are summarized in Table III. In comparison with the works of Nesbet and Chung, our energies are consistently 0.1 ± 0.02 a.u. higher except for the $^2S^e$ state of the third manifold where the difference is bigger. The relative energy spacings are fairly well-reproduced. Consequently we may attribute the energy differences of the known states largely to angular correlations, or equivalently, to the rovibrational motion of the electronic orbits. The near constant energy shift is likely a result of underestimating the radial correlation energy. The exceptional behavior of the $^2S^e$ state could be due to the particularly strong radial correlation in this state. Figure 7 maps the three manifolds of levels in a manner akin to Fig. 3. Only the three different manifolds are identifiable from the clusters. No l-type doublets are seen.

The states $^4P^e$ and $^2P^o$ in Fig. 7 follow the energy ordering of an oblate molecule in contrast to what was seen

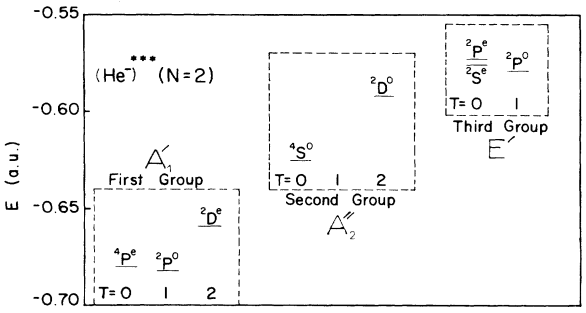

FIG. 7. Same as Fig. 3 for $N=2$ shell of He^-.

in Fig. 3 for the $N=3$ shell. This reversal could be due to the breakdown of treating triply excited states in the $N=2$ manifold as a symmetric top. It is worth checking by a more complete calculation whether the order of $^4P^e$ and $^2P^o$ follows the prediction of Fig. 3 or Fig. 5.

V. SUMMARY AND CONCLUSION

In this paper we have considered whether the molecular language will help the classification of triply excited states of atoms. We have proposed a model for the three-electron atom treating angular correlations adequately but leaving out radial correlations. By considering that the total angular momentum of a triply excited state has a quasi-invariant projection onto the symmetric axis of the body frame, we have been able to rearrange the energy levels into different manifolds of bending vibrational excitation, each manifold consisting of rotational levels similar to those of a symmetric top. How realistic is this model calculation compared to the actual atomic spectra of triply excited states? The answer to this question may have to await a fuller theoretical calculation as well as reliable experimental studies of a large number of resonances in the $N=3$ shell. We believe the present classification scheme will serve as useful guidance to the eventual understanding of the three-electron dynamics. Examining the details of and possible deviations from the molecular picture may similarly require a full analysis of accurate energy levels and wave functions. We expect from our earlier analysis of doubly excited states[1(a)] that the purity of the T quantum number serves as a measure of the effectiveness of the classification scheme.

Our analysis here has neglected radial correlations completely. To incorporate radial correlations, we need two additional quantum numbers conjugate to the two hyperangles in hyperspherical coordinates[7] (which are suited for describing the additional doubly degenerate stretching mode). A full treatment should then exhibit excitations in antisymmetric stretch modes like the "$-$" states of doubly excited atoms. Many of the states shown in Fig. 3 will autoionize. Nonetheless, the molecular modes should provide a scheme for classifying hyperspherical channels. The analysis of the three-electron correlations in real atoms will be a challenging problem for the years to come.

The present study is limited to the understanding of the

stationary states and is thus incapable of calculating excitation probabilities or treating decay processes. In view of the recent experimental analyses of the optical excitation functions[37–41] in

$$e+\mathrm{He}\rightarrow(\mathrm{He}^-)\rightarrow \underset{\mathrm{He}+h\nu}{\mathrm{He}^*}+e\ , \tag{33}$$

a physical theory of decay involving the temporary formation of triply excited states will be in good demand. To the authors' knowledge, there exists no comprehensive theory regarding this point.

Relevance of the present study is not limited to the isoelectronics of He^-. Atoms in which the outer three electrons are in the same shell are expected to display correlation effects noticeably. The isoelectronics of Al are such an example. The well-known $^2D^e$ resonance of Al is isomorphic to the $He^-(^2D^e)$ state of the first group of Fig. 3; both are formed by the strong mixing of the sp^2 and s^2d configurations.[42] There now exist some theoretical[43–45] and experimental studies[46] on similar systems, but the order of levels appears to change from one system to another significantly.[46] Unfortunately, in most atoms the presence of the inner-shell core complicates the treatment, thus much remains to be clarified. One fact we wish to point out in this connection is that the resonance positions[45] of C^- ($^4S^o$, $^2D^o$, $^2P^o$) appear in the order $^4S^o<{}^2D^o<{}^2P^o$ from lower to higher. The first two are sharp Feshbach-type resonances whilst the $^2P^o$ resonance is shapetype. In our language the former two resonances belong to the second group of Fig. 3, and the third one to the third group thereof. In the independent particle language, however, they all belong to the same configuration p^3. Let us note further that the energy order of $^4S^o$, $^2D^o$, and $^2P^o$ is consistent with Hund's rules. The point is that our present classification scheme enriches Hund's rules by permitting to compare different configurations, including strong mixings.

ACKNOWLEDGMENTS

We thank Professor U. Fano and Dr. M. Le Dourneuf for their continuing guidance and interest in the subject. Thanks are also due Dr. S. Leach, Dr. P. O'Mahony, Professor A. Defrance, and Dr. P. J. M. Van der Burgt for useful discussions. One of us, S. W., has received partial support from the Action Thématique Programmée "Physique Fondamentale" of the Centre National de la Recherche Scientifque (CNRS). One of us, C.D.L., is supported in part by the U. S. Department of Energy, Office of Basic Energy Sciences, Division of Chemical Sciences. The computation was carried out partly at the Centre Inter-Régional de Calcul Électronique in Orsay using computer time granted by the CNRS and partly at Kansas State University using the computing facility of the Physics Department. Work was also supported by a National Science Foundation–CNRS cooperative research program. "Equipe de Recherche 261 du CNRS" is at the Observatoire de Paris–Meudon.

[1](a) S. Watanabe and C. D. Lin, Phys. Rev. A **34**, 823 (1986); (b) C. D. Lin, *ibid.* **29**, 1019 (1984).
[2]J. H. Macek, J. Phys. B **1**, 831 (1968).
[3]C. D. Lin, Phys. Rev. A **10**, 1986 (1974).
[4]H. Klar and W. Schlecht, J. Phys. B **9**, 7699 (1976).
[5]C. H. Greene, Phys. Rev. A **23**, 661 (1981).
[6]U. Fano, Rep. Prog. Phys. **46**, 97 (1983) and references therein.
[7]S. Watanabe, M. Le Dourneuf, and L. Pelamourgues, J. Phys. (Paris) Colloq. **43**, C2-233 (1982).
[8]M. E. Kellman and D. R. Herrick, Phys. Rev. A **22**, 1536 (1980); J. Phys. B **11**, L755 (1978).
[9]D. R. Herrick, M. E. Kellman, and R. D. Poliak, Phys. Rev. A **22**, 1517 (1980).
[10]D. R. Herrick, Adv. Chem. Phys. **52**, 1 (1983).
[11]G. S. Ezra and R. S. Berry, Phys. Rev. A **28**, 1974 (1983) and references therein.
[12]S. I. Nikitin and V. N. Ostrovsky, J. Phys. B **18**, 4349 (1985).
[13]M. Barat (private communication).
[14]See, for example, C. D. H. Chisholm, *Group Theoretical Techniques in Quantum Chemistry* (Academic, New York, 1976), pp. 86 and 87.
[15]C. W. Clark and C. H. Greene, Phys. Rev. A **21**, 1786 (1980).
[16]See, for example, A. Messiah, *Quantum Mechanics* (Wiley, New York, 1958), Vol. II, p. 1104, Eq. (D-39); J. N. Murrell, S. F. A. Kettle, and J. M. Tedder, *Valence Theory* (Wiley, London, 1965), p. 99 or any standard text on group theory.
[17](a) See, for example, D. Papoušek and M. R. Aliev, *Molecular Vibrational Rotational Spectra* (Elsevier, New York, 1982), pp. 81 and 82; (b) G. Herzberg, *Molecular Spectra and Molecular Structure* (Van Nostrand, New York, 1959).
[18]See, for example, L. D. Landau and E. M. Lifshitz, *Quantum Mechanics* (Pergamon, Oxford, 1965), Vol. 3, p. 385.
[19]C. E. Kuyatt, J. A. Simpson, and S. R. Mielcezarek, Phys. Rev. **138**, A358 (1965); J. A. Simpson, M. G. Menendez, and S. R. Mielcezarek, *ibid.* **150**, 76 (1966).
[20]P. D. Burrow and G. J. Schulz, Phys. Rev. Lett. **22**, 1271 (1969).
[21]J. T. Grisson, R. N. Compton, and W. R. Garrett, Phys. Lett. **30A**, 117 (1969).
[22]I. Eliezer and Y. K. Pan, Theor. Chim. Acta. **16**, 63 (1970).
[23]D. E. Golden and A. Zecca, Phys. Rev. A **1**, 241 (1970).
[24]J. J. Quemener, C. Pagnet, and P. Marmet, Phys. Rev. A **4**, 494 (1971).
[25]C. A. Nicolaides and Y. Kominos, Phys. Rev. A **24**, 1103 (1981).
[26]L. Sanche and G. J. Schulz, Phys. Rev. A **5**, 1672 (1972).
[27]K. Smith, D. E. Golden, S. Ormonde, B. W. Torres, and A. R. Davies, Phys. Rev. A **8**, 3001 (1973).
[28]P. D. Marchand, Can. J. Phys. **51**, 814 (1973).
[29]A. J. Smith, P. J. Hicks, F. H. Read, S. Cvejanovic, G. C. M. King, J. Comer, and J. M. Sharp, J. Phys. B **7**, L496 (1974).
[30]S. Ormonde, F. Kets, and H. G. M. Heideman, Phys. Lett. **50A**, 147 (1974).
[31]M. Ahmed and Lipsky, Phys. Rev. A **12**, 1176 (1975).
[32]R. K. Nesbet, Bull. Am. Phys. Soc. **20**, 1471 (1975); Phys. Rev. A **14**, 1326 (1976).
[33]V. I. Safranova and V. S. Senaskenko, J. Phys. B **11**, 2623 (1978).

[34]K. T. Chung, Phys. Rev. A **20**, 724 (1979).
[35]C. A. Nicolaides, Y. Kominos, and D. R. Beck Phys. Rev. A **24**, 1103 (1981).
[36]M. Le Dourneuf and S. Watanabe, Dixième Colloque sur la Physique des Collisions Atomiques et Electroniques, Aussois (France), conférences invitées pp. 65–9 (1984) (unpublished).
[37]P. J. M. Van der Burgt, J. Van Eck, and H. G. M. Heideman, J. Phys. B **18**, 999 (1985); *ibid.* B **18**, L171 (1985).
[38]P. J. M. Van der Burgt, *Three-Electron Correlations in Electron-Helium Collisions,* Ph.D. thesis, Rijksuniversiteit Utrecht, Netherlands (1986).
[39]A. Defrance, J. Phys. B **13**, 1229 (1980).
[40]J. A. Baxter, J. Comer, P. J. Hicks, and J. W. Mc Conkey, J. Phys. B **12**, L355 (1979); **12**, 2031 (1979).
[41]H. G. M. Heideman, G. Nieuknis, and T. Van Ittersum, J. Phys. B **8**, L26 (1975).
[42]P. O'Mahony, Phys. Rev. A **32**, 908 (1985) and references therein.
[43]C. D. Lin, Astrophys. J. **187**, 385 (1974).
[44]M. Le Dourneuf, Vo Ky Lan, P. G. Burke, and K. T. Taylor, J. Phys. B **8**, 2640 (1975); K. T. Taylor, C. J. Zeippen, and M. Le Dourneuf, *ibid.* B **17**, L157 (1984).
[45]M. Le Dourneuf, Ph.D. thesis (Ecole Normal Superieure), Université Pierre et Marie Curie, 1976.
[46]G. K. James, L. F. Forrest, K. J. Ross, and M. Wilson, J. Phys. B **18**, 775 (1985) and references therein.